Production of branched tetraethers in the marine realm: Svalbard fjord sediments revisited

Emily Dearing Crampton-Flood [a,*], Francien Peterse [a], Jaap S. Sinninghe Damsté [a,b]

[a] *Department of Earth Sciences, Faculty of Geosciences, Utrecht University, Vening Meinesz Building A, 3584 CB Utrecht, the Netherlands*
[b] *Department of Marine Microbiology and Biogeochemistry, NIOZ Royal Netherlands Institute for Sea Research, and Utrecht University, 1790 AB Den Burg, Texel, the Netherlands*

ARTICLE INFO

ABSTRACT

Branched glycerol dialkyl glycerol tetraethers (brGDGTs) are bacterial membrane lipids thought to be predominantly produced on land. They are used as a terrestrial paleothermometer based on an empirical relation between their molecular composition and air temperature in surface soils worldwide. The proxy has been applied in continental margin sediments based on the assumption that all brGDGTs originate from land and are transported to marine sediments predominantly by rivers. However, this assumption has been challenged by the discovery of in situ brGDGT production in the coastal marine environment. To better understand marine brGDGT production, we examined newly collected marine surface sediments from the Krossfjorden and Kongsfjorden in Svalbard with a chromatography method to separate previously co-eluting 5- and 6-methylated brGDGT isomers. 'Living' intact polar lipid (IPL)-derived and 'fossil' core lipid (CL) brGDGTs were also studied for a subset of fjord sediments. The relative proportion of cyclopentane moieties in tetramethylated brGDGTs, used as indicator for brGDGT production in coastal marine settings, is much higher in the fjord sediments ($\#rings_{tetra}$ = 0.65–0.93 for CL and 0.24–0.79 for IPL-derived brGDGTs) compared to those in nearby soils ($\#rings_{tetra}$ = 0.00–0.37), and confirms the predominantly marine source of the brGDGTs in the fjord. Surprisingly, however, IPL-derived brGDGTs have a substantially lower $\#rings_{tetra}$ (up to 0.52 offset) compared to that of CL-brGDGTs in the same sediment. This suggests that brGDGTs are produced in situ in different distributions throughout the year, of which the CL distribution in the sediment is an integrated signal. The offset in $\#rings_{tetra}$ between IPL-derived and CL brGDGTs varies between 0.15 and 0.52 and increases towards the open ocean, possibly linking brGDGT production to the natural salinity gradient and associated microbial community changes.

1. Introduction

Branched glycerol dialkyl glycerol tetraethers (brGDGTs) are membrane lipids produced by bacteria that thrive in soils and peats (Weijers et al., 2007a; Peterse et al., 2012; De Jonge et al., 2014a; Naafs et al., 2017a) worldwide. Specific brGDGT structures are distinguished by the varying number of methyl branches (4–6) and cyclopentane moieties (0–2) that are present in the interior alkyl chains (see Appendix for molecular structures). Furthermore, the position of the outer methyl branches in the pentamethylated and hexamethylated brGDGTs can vary from the fifth to the sixth, and even seventh position on the alkyl chain, giving rise to structural isomers, referred to as 5-, 6-, and 7-methylated brGDGTs

(Sinninghe Damsté et al., 2000; De Jonge et al., 2013; Ding et al., 2016). Variations in the degree of methylation of brGDGTs (methylation of branched tetraethers, MBT) in a set of globally distributed soils have been linked to mean annual air temperature (MAAT; Weijers et al., 2007a; De Jonge et al., 2014a), whereas the degree of cyclisation (Weijers et al., 2007a; Peterse et al., 2012), as well as the position of the outer methyl branch (De Jonge et al., 2014a), are related to soil pH. Subsequently, these relations have resulted in global transfer functions that are employed as a terrestrial paleothermometer (De Jonge et al., 2014a; Naafs et al., 2017b). The first proof of concept of the proxy resulted in a temperature record for the last deglaciation in equatorial Africa (Weijers et al., 2007b). Subsequently, it has been applied to reconstruct temperatures in the mid- to high-latitudes during the early Paleogene (e.g., Weijers et al., 2007c; Inglis et al., 2017; Naafs et al., 2018), and the Arctic in the Pliocene (e.g., Ballantyne et al., 2010; Keisling et al., 2017), among others.

---

* Corresponding author at: School of Earth and Environmental Sciences, The University of Manchester, Williamson Building, M13 9QQ Manchester, UK.

E-mail address: Emily.dearingcrampton-flood@manchester.ac.uk (E. Dearing Crampton-Flood).

Application of the brGDGT-based paleothermometer on continental margin sediments relies on the underlying assumption that soil- and peat-derived brGDGTs are washed into rivers and delivered into the marine realm. This assumption has been challenged by the recent findings that brGDGT production also takes place in situ in rivers (Zell et al., 2013a, 2013b; De Jonge et al., 2014b), lakes (Tierney and Russell, 2009; Sinninghe Damsté et al., 2009; Weber et al., 2015, 2018), and continental margins (Peterse et al., 2009; Zhu et al., 2011; Zell et al., 2014a, 2014b; De Jonge et al., 2015; Liu et al., 2014, Xie et al., 2014; Sinninghe Damsté, 2016), altering the initial brGDGT signal produced in soils. However, the specific organism(s) responsible for producing brGDGTs remain ambiguous. To date, various subdivisions of the phylum Acidobacteria, an abundantly occurring group of bacteria in soils and peats, have been identified as producers of an assumed essential building block of brGDGTs, i.e. *iso*-diabolic acid, and a few species actually produce brGDGT Ia (Sinninghe Damsté et al., 2011, 2014, 2018). However, recent work has proposed that the search for the biological sources of brGDGTs should be extended to other bacterial phyla, due to the absence of the gene cluster in many subdivisions of Acidobacteria that is responsible for the formation of the ether-bound variety of *iso*-diabolic acid, the surmised building block of brGDGTs (Sinninghe Damsté et al., 2018). Identifying the specific bacteria that produce brGDGTs in marine and terrestrial settings would likely facilitate the separation of brGDGTs with an aquatic from those with a terrestrial source in coastal marine or lacustrine sediments. Instead, different sources are currently identified solely based on empirical brGDGT distributions.

Evidence of in situ marine brGDGT production was first reported for the Kongsfjorden and Krossfjorden of Svalbard (Peterse et al., 2009), where the concentration of brGDGTs in fjord sediments increased with distance from the land, opposite to the expected trend based on a soil origin for the brGDGTs. This trend is also in contrast to previous studies that have used brGDGTs to trace fluvially discharged soil OC into the marine realm (Hopmans et al., 2004; Herfort et al., 2006; Kim et al., 2006, 2007). Furthermore, brGDGTs in the Svalbard fjord sediments contained more cyclopentane moieties than those in the Svalbard soils. This contrast led to the conclusion that at least part of the brGDGTs in the fjord sediments were produced in situ, and thus MAAT reconstructions using these sediments would be unreliable (Peterse et al., 2009). A similarly high proportion of ring-containing brGDGTs in modern coastal zones was later observed in the East China Sea, the Portuguese continental margin, and the Berau Delta in Indonesia (Zhu et al., 2011; Zell et al., 2015; Sinninghe Damsté, 2016). Additionally, a high proportion of ring-containing brGDGTs is also observed in distal marine surface sediments (Weijers et al., 2014). These observations led to the use of the weighted number of rings of the tetramethylated brGDGTs, quantified as #rings$_{tetra}$, as an indicator for in situ marine brGDGT production. Based on these three sites, a threshold of #rings$_{tetra}$ > 0.7 has been proposed as an indicator for a predominantly marine source of brGDGTs in marine sediments (Sinninghe Damsté, 2016).

A marine contribution impedes the use of the brGDGT-based paleothermometer as a terrestrial temperature proxy, due to the fact that the calibration is based upon a global soil dataset (De Jonge et al., 2014a). Therefore, Dearing Crampton-Flood et al. (2018) recently proposed a method to resolve the influence of mixed brGDGT sources in marine sediments on continental temperature reconstruction. This method uses an end-member mixing model to disentangle the sources of brGDGTs in the paleo-record based on #rings$_{tetra}$. Subsequently, a separate coastal marine transfer function was used to subtract the marine contribution from the terrestrial temperature signal. This correction method thus expands the use of brGDGTs as a continental paleothermometer.

However, the drivers of marine in situ brGDGT production, including temporal and spatial variations, still remain uncertain.

To further elucidate trends in marine in situ brGDGT production, we analysed newly collected surface sediments collected from the same locations as the surface sediments in Peterse et al. (2009) exactly one year later, using the new chromatography method to separate 5- and 6-methylated brGDGT isomers (cf. De Jonge et al., 2014a; Hopmans et al., 2016). Due to the presumably low sedimentation rate in the fjords, the detection of inter-annual changes in brGDGT distributions between the 2007 and 2008 sediments is presumed to be minimal. To specifically investigate the signature of in situ produced brGDGTs in marine settings, a subset of the sediments was separated into intact polar lipid (IPL)-derived and core lipids (CLs) using column chromatography and analysed accordingly. IPLs are structurally different from CLs as they contain a polar headgroup (Koga et al., 1993). IPL-derived lipids are considered as biomarkers for living biomass, as the headgroup is thought to be rapidly lost upon cell death, leaving the 'fossil' core lipid structure (White et al., 1979). Following this approach, brGDGT distributions from both 'living' organisms and the pool of 'fossil' brGDGTs stored in sediments can be directly compared. The results are discussed in context with the hydrological conditions of the Kongsfjorden and Krossfjorden fjords.

2. Material and methods

2.1. Environmental setting and fjord hydrogeography

The environmental setting of Svalbard and that of Kongsfjorden and Krossfjorden are described in detail in Peterse et al. (2009). In short, the surface current influencing the west coast of Spitsbergen is the West Spitsbergen Current (WSC; Fig. 1A), whose core is composed of Atlantic Water (AW). This relatively warm and saline AW leads to largely ice-free conditions throughout the year on the west coast of Spitsbergen. In contrast, the east coast is characterized by cooler conditions due to the influence of the colder East Spitsbergen Current (ESC, Fig. 1A). In Kongsfjorden and Krossfjorden, two water masses create a hydrogeographical gradient: the relatively warm, saline AW fed in by the WSC, and the tidewater glaciers on land whose input is characterized by cooler, fresh water. The interaction between these two water masses leads to large intra-annual hydrological changes which strongly affect the variability of fauna in the fjords and the nearby coastal shelf (Conte et al., 2018; Jernas et al., 2018). The Atlantic water mainly enters Kongsfjorden in the summer, although episodic intrusions have also been detected in winter (Svendsen et al., 2002; Jernas et al., 2018).

On average, the surface salinity varies from 30 g kg^{-1} in the innermost fjord areas (Svendsen et al., 2002) to 35 g kg^{-1} out towards the mouth and the shelf area (Jernas et al., 2018). In the Kongsfjorden, and by extension the neighbouring Krossfjorden, temperature and salinity gradients can vary inter-annually, as well as sediment supply and turbidity of water close to the glacier terminus (Svendsen et al., 2002; Jernas et al., 2018). The water depth in the two fjords varies from less than 100 m deep in the inner part of Kongsfjorden to 400 m at the intersection of the Kongsfjorden and Krossfjorden (Hop et al., 2002). Out toward the open ocean the depth decreases slightly again to around 200–300 m (Hop et al., 2002). Sea surface water temperatures in August/September in the fjords range from 5 to 7 °C (Jernas et al., 2018). The bottom water temperatures are usually stable around 2–3 °C (Jernas et al., 2018). The MAAT for Ny Ålesund, at the interior of the Kongsfjorden, is –5.8 °C (Birks et al., 2004). The sediment accumulation rate in Kongsfjorden changes from 20000 g m^{-2} yr^{-1} in the inner fjord to 1800–3800 g m^{-2} yr^{-1} in the central fjord, and finally to 200 g m^{-2} yr^{-1} in the outer fjord (Svendsen et al., 2002).
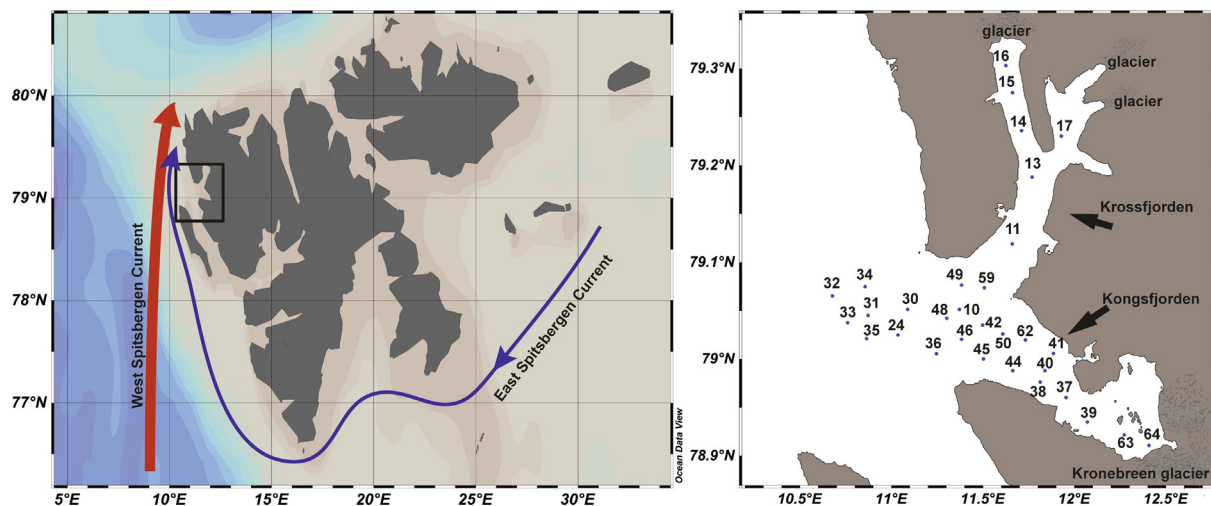
Fig. 1. Map showing: (A) Svalbard and relevant ocean currents, and (B) locations of marine surface sediment samples (2008 cruise) in Kongsfjorden and Krossfjorden. The inset in (A) shows the location of the fjords on Svalbard. For an overview of the exact locations of the sampling stations for the 2007 and 2008 cruises, see Supplementary Table S1. Maps were constructed using the Ocean Data View (odv.awi.de) software.

2.2. Sampling and collection of environmental variables

The soil (n = 9) and surface sediment (n = 29; 0–1 cm) sampling on the R/V *Lance* cruise in September 2007, as well as the specifications of the sites and bulk properties of the samples, have been described in Peterse et al. (2009). Additional marine surface sediments (n = 31; 0–1 cm) were collected in August 2008, with a multicorer from the R/V *Lance* at approximately the same locations as in 2007 (Fig. 1B; Supplementary Table S1). All sediments were stored on board at −20 °C, transported to the Royal NIOZ on dry ice, and stored at −40 °C until further analysis.

Physical oceanographic properties including temperature, salinity, and pressure in the water column were measured with a CTD (Seabird SBE 9111 plus) during the 2007 and 2008 cruises at a select number of sample locations prior to multicorer sampling.

2.3. GDGT extraction

The extraction method for the soils and sediments from the 2007 cruise is described in Peterse et al. (2009). Freeze-dried and powdered surface sediments from the 2008 cruise were extracted in the same manner, using a DIONEX accelerated solvent extractor (ASE 200) with a mixture of dichloromethane (DCM):methanol (MeOH) (9:1, v/v) at 100 °C and 7.6×10^6 Pa for 3 back-to-back extractions of 5 min. The addition of an internal standard (C_{46}; Huguet et al., 2006), subsequent column fractionation, and filtration steps are identical to those of Peterse et al. (2009). In brief, extracts were separated into apolar and polar fractions over an activated Al_2O_3 column using hexane:DCM (9:1, v/v), and MeOH: DCM (1:1, v/v), respectively. Then all polar fractions were dissolved in hexane:isopropanol (99:1, v/v), and filtered through a 0.45 μm PTFE filter.

In order to quantify and examine the distribution of the IPL-derived brGDGTs, which cannot be recovered using ASE techniques, a spatially evenly distributed subset of samples (n = 14, see Supplementary Table S1) of the freeze-dried sediments from the 2008 cruise was extracted with a modified Bligh-Dyer extraction (cf. Pitcher et al., 2009). Samples were extracted (3×) ultrasonically using a single-phase solvent mixture of MeOH/DCM/phosphate buffer 10:5:4 (v/v/v) for 10 min. DCM and phosphate buffer were added to the combined extracts to obtain a new mixture of 1:1:0.9 (v/v/v) and achieve phase separation. The DCM phase was collected and passed over a silica column (modified procedure from Pitcher et al., 2009) to obtain IPL and CL fractions using hexane/ethyl acetate (1:1, v/v) and MeOH as eluents, respectively. In order to cleave off the head groups on the IPLs, the IPL fraction was refluxed for 2 h with 1.5 N HCl in MeOH. An internal standard (Huguet et al., 2006) was added to the CL and IPL-derived GDGT fractions before filtration over a 0.45 μm PTFE filter as above.

2.4. GDGT analysis

Polar fractions containing brGDGTs from the Svalbard soils were previously re-analysed to separate 5- and 6-methyl isomers by De Jonge et al. (2014a) and included in the global soil dataset. Similarly, the marine sediments from the 2007 cruise were re-analysed for 5- and 6-methyl brGDGTs earlier by Sinninghe Damsté (2016). The marine sediments collected in 2008 are novel to this study, and were also analysed according to the latest method of Hopmans et al. (2016) using an Agilent 1260 Infinity ultra high performance liquid chromatography (UHPLC) coupled to an Agilent 6130 single quadrupole mass detector. Two silica Waters Acquity UPLC BEH Hilic (1.7 μm, 2.1 mm × 150 mm) columns with a guard column at 30 °C were used for separation. Injection volume for each sample was 10 μL. An isocratic gradient was used, starting with 82% A and 18% B at a flow rate of 0.2 ml/min for 25 min, then a linear gradient to 70% A and 30B for 25 min, where A = hexane and B = hexane/isopropanol (9:1, v/v). The following source conditions were used for the atmospheric pressure chemical ionisation (APCI): gas temperature 200 °C, drying gas (N_2) flow 6 L/min, vaporizer temperature 400 °C, nebulizer pressure 25 psi, capillary voltage 3500 V, corona current 5.0 μA. Selected ion monitoring (SIM) mode was used to detect the $[M−H]^+$ ions of GDGTs at m/z 1292, 1050, 1048, 1046, 1036, 1034, 1032, 1022, 1020, 1018 and at 744 for the internal standard.

The #rings for the 5-methyl brGDGTs was calculated as follows (Sinninghe Damsté, 2016):

$$\#rings_{tetra} = ([Ib] + 2 \times [Ic])/([Ia] + [Ib] + [Ic]) \quad (1)$$

$$\#rings_{penta} = ([IIb] + 2 \times [IIc])/([IIa] + [IIb] + [IIc]) \quad (2)$$

$$\#rings_{hexa} = ([IIIb] + 2 \times [IIIc])/([IIIa] + [IIIb] + [IIIc]) \quad (3)$$

in which the roman numerals refer to the molecular structures in the Appendix. The #rings for the 6-methyl isomers was calculated

following the same equations, only using the molecular structures indicated with a prime symbol. The relative contribution of 6-methyl brGDGTs, i.e. the degree of isomerization, is quantified in the isomer ratio (IR), calculated according to the following equation (De Jonge et al., 2014b, 2015):

$$IR = \frac{[IIa'] + [IIb'] + [IIc'] + [IIIa'] + [IIIb'] + [IIIc']}{[IIa'] + [IIb'] + [IIc] + [IIIa'] + [IIIb'] + [IIIc'] + [IIa] + [IIb] + [IIc] + [IIIa] + [IIIb] + [IIIc]} \qquad (4)$$

The IR_{penta} and IR_{hexa} variants only use the pentamethylated and hexamethylated groups of brGDGTs, respectively.

The BIT index was calculated as follows, and explicitly includes both the 5- and 6-methyl brGDGT isomers (Hopmans et al., 2004):

$$BIT = \frac{Ia + IIa + IIa' + IIIa + IIIa'}{IV + Ia + IIa + IIa' + IIIa + IIIa'} \qquad (5)$$

3. Results

3.1. BrGDGTs in ASE extracts of Kongsfjorden and Krossfjorden sediments

BrGDGTs in the ASE extracted sediments from Kongsfjorden and Krossfjorden collected in 2007 are most abundant in hexamethy-lated brGDGTs (43.7 ± 7.8%), followed by penta- (28.9 ± 2.8%) and tetramethylated brGDGTs (27.5 ± 5.5%; Supplementary Table S1). Those collected in 2008 are dominated by both penta- and hexam-ethylated brGDGTs (35.6 ± 2.3% and 34.6 ± 4.8%), followed by tetramethylated brGDGTs (29.8 ± 3.3%). In both years, the hexam-ethylated IIIa′ is the most abundant brGDGT (24.6 ± 6.6% for sedi-ments collected in 2007, 19.2 ± 4.1% for those collected in 2008; Fig. 2D–E). The average fractional abundances of 6-methyl brGDGTs in the surface sediments comprise on average 34.5 ± 4.0% in 2007, and 36.0 ± 5.9% of the total brGDGT pool in 2008, and are not significantly different between years (*t*-test, p = 1). As a result, the IR is similar for both years, and was 0.35–0.55 in 2007 and 0.30–0.54 in 2008 (Fig. 3A). More specifically, the IR_{penta} was 0.29–0.52 in 2007, and 0.35–0.68 in 2008. The IR_{hexa} was 0.18–0.55 in 2007 and 0.39–0.70 in 2008. The $\#rings_{tetra}$ was 0.66–1.00 in 2007 and 0.56–0.92 in 2008. The $\#rings_{penta}$ was 0.65–0.96 and 0.51–1.00 for the 5- and 6-methyl varieties in 2007, and between 0.50–0.94 and 0.45–0.94 in 2008 (Fig. 3C). The $\#rings_{hexa}$ was never higher than 0.19 for both the 5- and 6-methyl varieties in either year. The spatial variation of the #rings is similar in both years. Focussing on the surface sediments from
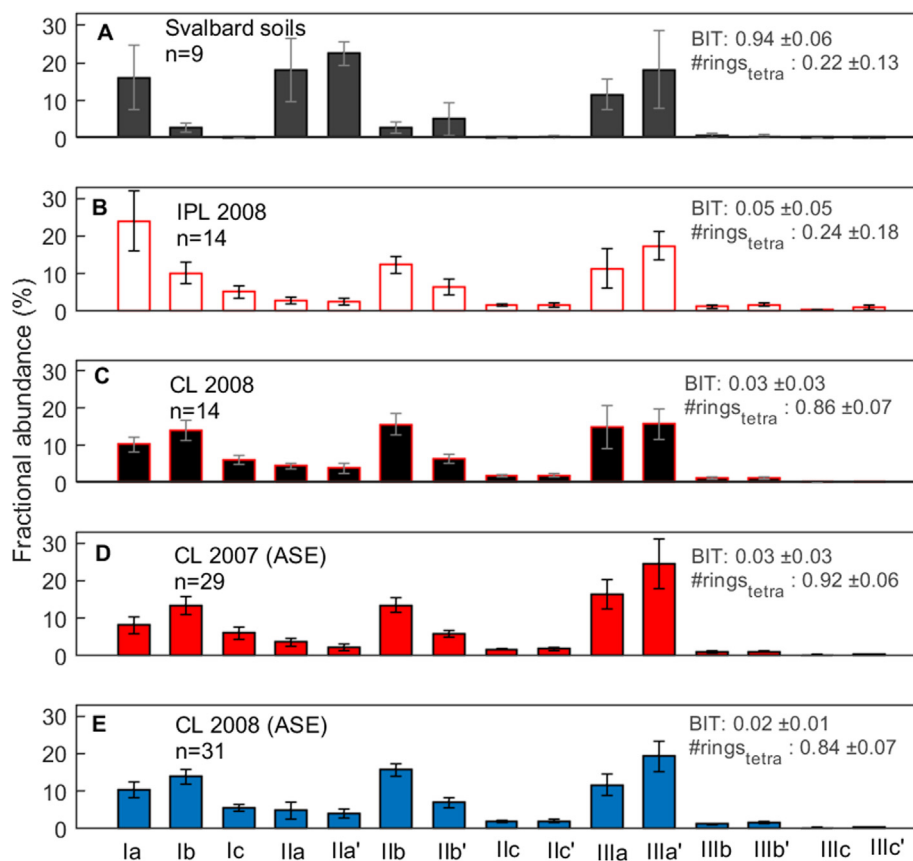

Fig. 2. Average fractional abundance of brGDGTs in Svalbard soils (A; De Jonge et al., 2014a) and fjord sediments (B–E; Sinninghe Damsté, 2016; this study). Intact polar lipid (IPL)-derived (B) and core lipid (CL; C) brGDGT fractional abundances (this study) are derived from Bligh-Dyer extraction and workup, and are shown for a subset of the 2008 cruise surface sediments. The CL fractional abundances in the soil and fjord sediments from the 2007 (D) and 2008 (E) cruises data are derived from accelerated solvent extraction (ASE). Error bars indicate standard deviation.

2008, the #rings$_{tetra}$ was generally lower (0.77 ± 0.12) in the inner fjords, increases towards the intersection of the fjords (0.88 ± 0.03), and then slightly decreases towards the open ocean (0.83 ± 0.01; Fig. 4B). In general, the highest values of #rings$_{tetra}$ occur around the mouth of both fjords. There are two locations where #rings$_{tetra}$ is substantially lower: close to the Kronebreen glacier (NP-08-16-64) and at a near-shore location in the Krossfjorden (NP-08-16-14). These sediments are also characterized by a slightly higher BIT index of 0.05 and 0.04, respectively, as opposed to values below 0.03 for the other sites (Supplementary Table S1).

3.2. CL and IPL-derived brGDGTs in Bligh-Dyer extracts of Kongsfjorden and Krossfjorden sediments

A selection of the Kongsfjorden and Krossfjorden sediments (n = 14) obtained in 2008 was extracted using Bligh-Dyer type extraction to separate IPL from CL brGDGTs. The brGDGT distributions of the CL fraction from the Bligh-Dyer extraction and the ASE-derived brGDGTs should theoretically be the same, although the different extraction techniques may result in minor differences for the CL GDGTs (Lengger et al., 2012). Nevertheless, the fractional abundances of CL brGDGTs in the fjord sediments that were obtained after extraction using both ASE and Bligh-Dyer techniques are not significantly different (t-test, p > 0.05 for all brGDGTs). Indeed, CL brGDGTs in the Bligh-Dyer fractions are also dominated by both penta- (35.0 ± 2.8%) and hexamethylated brGDGTs (34.4 ± 7.0%), followed by tetramethylated brGDGTs

(30.7 ± 5.0%), with IIIa′, IIb, and IIIa as most abundant compounds (15.8 ± 4.0%, 15.7 ± 2.7%, and 15.0 ± 5.9%, respectively; Fig. 2C; Supplementary Table S1). Also, the IR compares well with that of the ASE-extracted CLs, and ranges from 0.32 to 0.51, with IR$_{penta}$ values of 0.34–0.61 and IR$_{hexa}$ values of 0.39–0.75 (Fig. 3A). The #rings$_{tetra}$ and #rings$_{penta}$ range between 0.65 and 0.93, the #rings$_{penta-6me}$ ranges between 0.48 and 0.95, whereas the #rings$_{hexa}$ is again always below 0.19 (Fig. 3C). The #rings$_{tetra}$ values follow the same spatial pattern as that of the ASE-extracted brGDGTs.

The IPL-derived brGDGTs make up only a small part (5.8% on average) of the total brGDGT pool in the sediments, with a large range of variation (1.7–25.8%). The site with the highest %IPL was located just outside the fjord mouth, whereas %IPL remained fairly low (<8%) in other areas (Fig. 4A). The distribution of the IPL-derived brGDGTs differs from that of the CLs and is characterized by a higher contribution of tetramethylated brGDGTs (39.3 ± 5.9%), followed by hexa- (33.0 ± 6.1%) and pentamethylated brGDGTs (27.7 ± 4.8%; Fig. 2B). BrGDGT Ia is the major compound (24 ± 8.1%), and brGDGT IIIa′, which dominates all CL fractions, is only the second most abundant IPL-derived brGDGT (17.3 ± 3.8%). The IR of the IPL-derived brGDGTs is 0.37–0.61, with IR$_{penta}$ ranging from 0.34 to 0.61, and IR$_{hexa}$ from 0.39 to 0.75 (Fig. 3A). The #rings$_{tetra}$ (0.24–0.79) is overall lower than that of the CLs. In contrast, the #rings$_{penta}$ is high for all sediments examined, being 0.78–1.0 and 0.61–1.0 for the 5- and 6-methyl isomers, respectively (Fig. 3C). The #rings$_{hexa}$ for the IPL-derived brGDGTs is low (0.09–0.28 and 0.08–0.35 for the 5- and 6-methylated isomers,
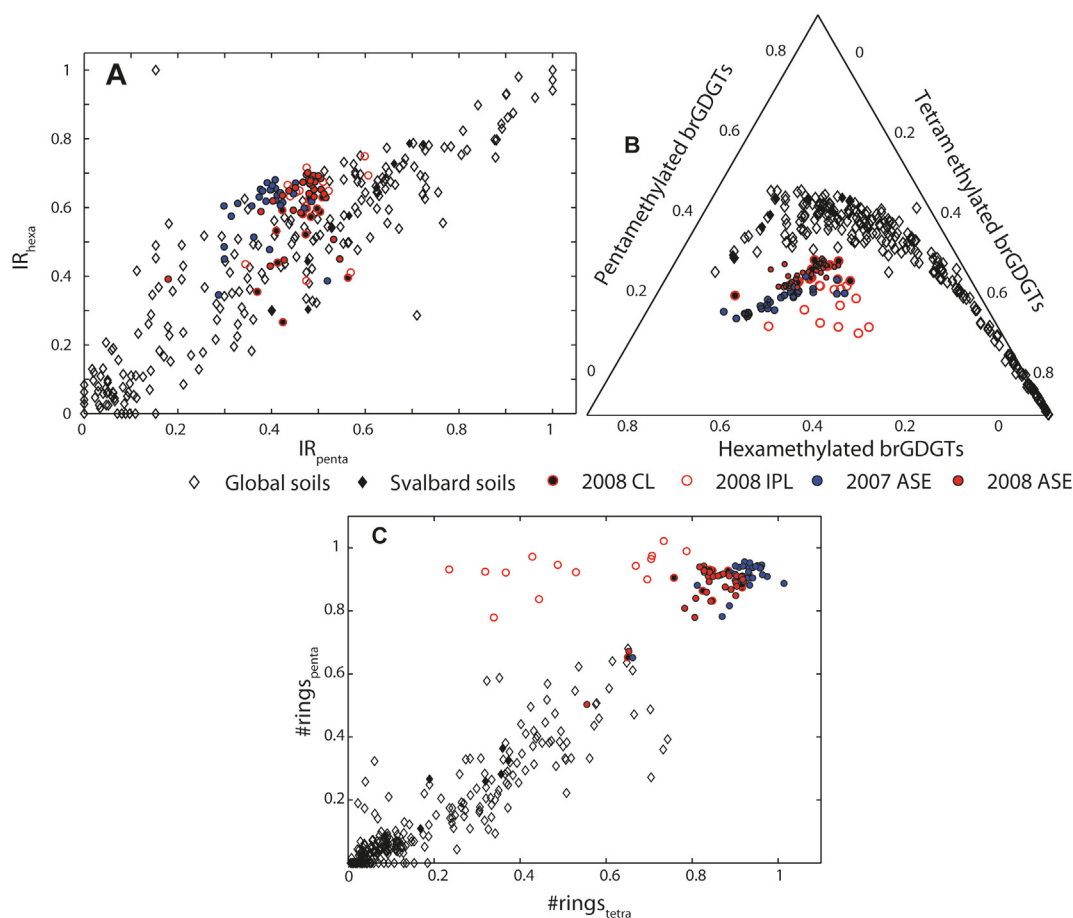

Fig. 3. (A) The isomer ratio (IR) of penta- vs hexamethylated brGDGTs, (B) ternary plot showing brGDGT distributions, and (C) the degree of cyclisation (#rings) of tetra- vs pentamethylated 5-methyl brGDGTs in Svalbard fjord sediments collected in 2007 (Sinninghe Damsté, 2016) and 2008 (this study), with IPL-derived and CL lipids distinguished (this study). BrGDGTs in soils (open diamonds) from the global soil calibration set (De Jonge et al., 2014a) are plotted for comparison. The Svalbard soils (part of the global soil calibration set) are denoted by black diamonds. (For interpretation of the colors in the figure(s), the reader is referred to the web version of this article.)
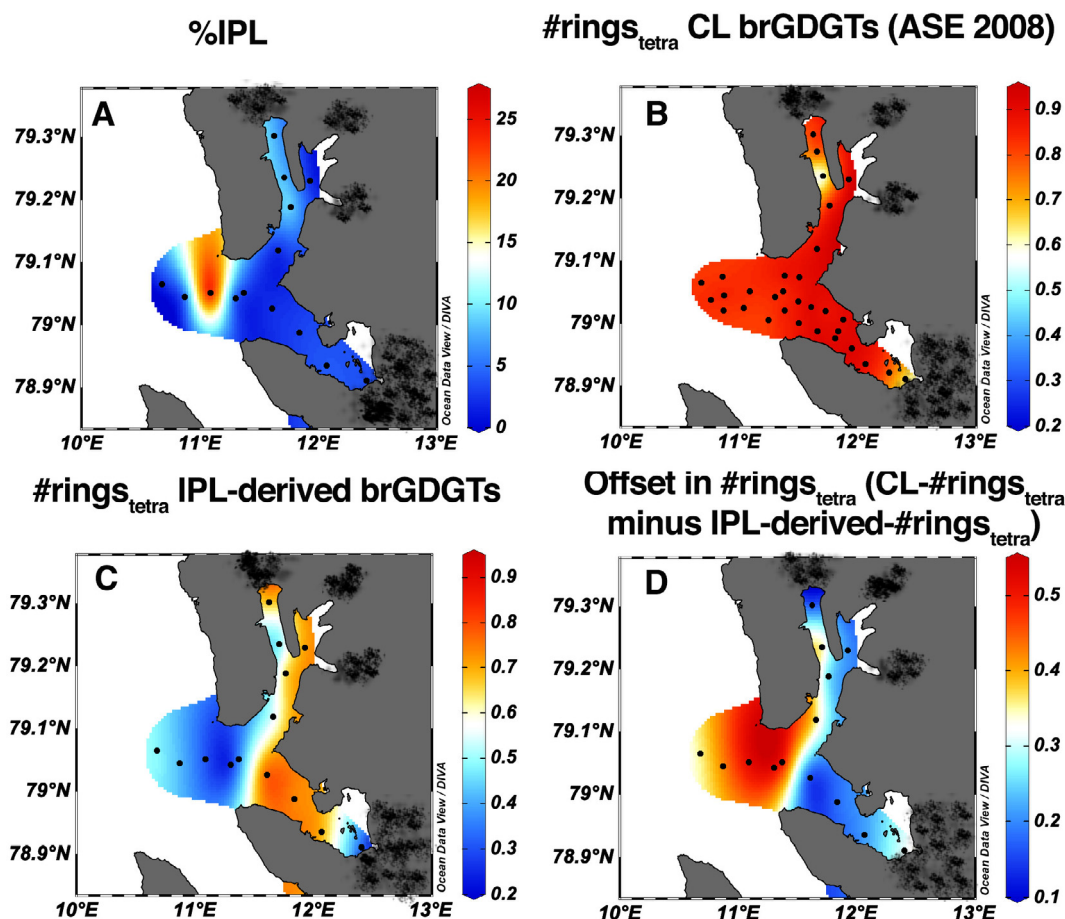
Fig. 4. The spatial distribution of: (A) the contribution (%) of the intact polar lipid (IPL)-derived brGDGTs to the total branched GDGT pool in Svalbard marine sediments. Spatial variation of brGDGT distributions expressed in the $\#rings_{tetra}$ for (B) core lipids (CLs) and (C) intact polar lipid (IPL)-derived brGDGTs in Svalbard marine sediments collected in 2008, and (D) the offset in $\#rings_{tetra}$ between CL and IPL-derived brGDGTs. Note that the same scale is used in panels (B) and (C) to facilitate direct comparison. All data presented are from marine sediments obtained during the 2008 cruise (Supplementary Table S1). The hatched black texture indicates the presence of glaciers. Surface plots were constructed using the Ocean Data View (odv.awi.de) software. DIVA (Data-Interpolating Variational Analysis) gridding was used to grid the fields of observations, using the default settings in Ocean Data View. (For interpretation of the colors in the figure(s), the reader is referred to the web version of this article.)

respectively), as observed for all other Svalbard brGDGT fractions. The spatial variation in the $\#rings_{tetra}$ of the IPL-derived brGDGTs follows that of the CL brGDGTs, although the amplitude of change is much larger (Fig. 4C). The highest values again occur in the mouth/interior part of the fjords, but decrease toward the open ocean. In front of the Kronebreen glacier, the $\#rings_{tetra}$ of the IPL-derived brGDGTs is relatively low (0.34), but not the lowest (0.24) in the stations considered, which occurs at the mouth of the fjords at station NP-08-16-48 (Fig. 4C).

4. Discussion

4.1. Provenance of brGDGTs in Svalbard fjord sediments

Svalbard soils contain relatively high amounts of 6-methylated brGDGTs (average 47 ± 13% of the total brGDGT pool) compared to most of the soils from the global soil dataset of De Jonge et al. (2014a; 23 ± 22%). The maximum proportion of 6-methylated brGDGTs in any soil from the global dataset is for MP4 at Svalbard (63%). This fits with the generally alkaline pH of most of the Svalbard soils (pH > 7 in 6 out of 9 soils; Peterse et al., 2009), as the contribution of 6-methylated brGDGTs, captured in the IR (0.37–0.73 for the Svalbard soils), generally increases with soil pH (De Jonge et al., 2014a). Although the IR of the brGDGTs in the fjord

sediments mostly falls within the range of that in soils, albeit in the lower part (Fig. 3A), the brGDGT distribution differs substantially from those in the soils (Fig. 2). This is particularly visible in the anomalously high proportion of ring-containing brGDGTs in the fjord sediments compared to that in soils. This offset was previously used as evidence by Peterse et al. (2009) of aquatic in situ production of brGDGTs in the Krossfjorden and Kongsfjorden sediments collected in 2007. The brGDGT distribution in the fjord sediments collected in 2008 show a similar distribution (Fig. 2), indicating that the peculiar distribution of brGDGTs in the fjord sediments cannot be attributed to inter-annual variation in soil input.

Sinninghe Damsté (2016) used a ternary diagram with the fractional abundances of tetra-, penta-, and hexamethylated brGDGTs to illustrate that certain marine sediments, including those from Svalbard (2007 cruise), plot offset from the global soils. The author proposed that an increasing offset relative to global surface soils reflects an increasing contribution of in situ produced brGDGTs. The Svalbard fjord sediments collected during the 2008 cruise plot in the same area as the 2007 cruise sediments in the ternary diagram of Sinninghe Damsté (2016), and thus confirm the primarily marine source of brGDGTs in Svalbard fjord sediments (Fig. 3B). In fact, the Svalbard fjord sediments show the largest offset so far to the soils of all modern continental margin sediments analysed with the new chromatography method. This is also reflected in the high

values for #rings$_{tetra}$ and #rings$_{penta}$ in these sediments in both 2007 (0.92 ± 0.06 and 0.90 ± 0.06, respectively; Sinninghe Damsté, 2016) and 2008 (0.86 ± 0.06 and 0.89 ± 0.06, respectively). These values are exceptionally high compared to those for Svalbard soils (Fig. 3C), as well as those in the global dataset, where #rings$_{tetra}$ and #rings$_{penta}$ range from 0.0 to 0.74, but have a median value of 0.12 (De Jonge et al., 2014a; Fig. 3C). As a result, the brGDGT signature from Svalbard has been used as a marine end-member to assess the qualitative contributions of soil-derived and marine in situ produced brGDGTs in a Pliocene sediment sequence from the Netherlands (Dearing Crampton-Flood et al., 2018), as well as in Baltic Sea Holocene sediments (Warden et al., 2018).

4.2. IPL-derived vs CL brGDGTs in Svalbard fjord sediments

To elucidate the presence and behaviour of the active community of brGDGT producers in the fjord sediments, we analysed IPL-derived brGDGTs, assuming that they mostly reflect the brGDGT of living biomass and thus of the brGDGT-producers in marine sediments. The relative distribution of IPL-derived brGDGTs in the fjord sediments differs from that of the CLs, and is characterized by a higher fractional abundance of brGDGT Ia in the IPL-derived pool (Fig. 2). This leads to a different order of fractional abundance of the tetramethylated brGDGTs; where Ib > Ia in the CL pool, and Ia > Ib for IPL-derived brGDGTs. Consequently, the #rings$_{tetra}$ of IPL-derived brGDGTs is substantially lower than that of the CLs in the same sediment and can differ up to 0.52 (Fig. 4D). Intriguingly, the #rings$_{penta}$ remains high for both CL and IPL-derived brGDGTs (Fig. 3C), indicating that #rings changes independently for tetra- and pentamethylated IPL-derived brGDGTs. Regardless, the higher #rings for both CL and IPL-derived brGDGTs in the fjord sediments compared to that in soils indicates that the discrepancy in composition between the CL and IPL-derived brGDGTs cannot be attributed to seasonally varying input sources (i.e. terrestrial vs marine). This suggests that the IPL-derived brGDGTs should reflect the membrane composition of the dominant microbial community present in the sediment at the time of collection, i.e. August/September. The CL signature should then represent an integration of long-term production throughout the year. The higher fractional abundance of brGDGT Ia in the IPL-derived pool could then be explained by Atlantic Water that enters the fjord in the summer (i.e. at the time of sampling). This warmer water can introduce a warm bias to the 'living' brGDGT signal either directly, due to membrane adaptation by their producers and/or a change in the dominant brGDGT-producing community, or indirectly, as a result of the introduction of a different brGDGT-producing microbial community with this water mass. Indeed, in August 2008 the sea surface temperatures at the entrance of the fjords is ~5 °C, which is ~2 °C warmer than waters near the Kronebreen glacier terminus (Supplementary Table S2). The difference in IPL-derived and CL signatures implies that 'living' brGDGTs likely vary in distribution over the season. Interestingly, this finding suggests that brGDGT-producers in the marine environment are more sensitive to seasonally changing environmental conditions than in soils, where seasonal patterns are absent in IPL-derived brGDGTs (Weijers et al., 2011).

4.3. Spatial variation in #rings

The #rings$_{tetra}$ values for CL brGDGTs in the fjord sediments follows a distinct spatial pattern (Fig. 4B), where #rings$_{tetra}$ initially increases on the coastal shelf (away from shore), and then decreases slightly towards the open ocean. This pattern is similar to what has been observed in the Berau delta, the East China Sea, and the Portuguese Margin (Zhu et al., 2011; Zell et al., 2015; Sinninghe Damsté, 2016). At these sites, the highest values of #rings$_{tetra}$ occur at 50–300 m water depth, suggesting that those depths are the most suitable for in situ brGDGT production (Sinninghe Damsté, 2016). The water depth in almost the entire Kongsfjorden-Krossfjorden system (average depths of 50 m in the inner glacial bays and ~400 m at the outer basins; Zhu et al., 2014) falls in this range. In particular, the highest values of #rings$_{tetra}$ (>0.9) in the fjords are found in the outer basin fjord area in the depth range of 270–310 m (Fig. 4B). At slightly deeper sites outside the mouth of the fjords and into the open ocean, the #rings$_{tetra}$ decreases slightly, but is still >0.8. The minor decrease in #rings$_{tetra}$ towards the open ocean (from 0.88 at the mouth of the fjords to 0.83 at the open ocean in the 2008 sediments) corresponds with depths at the deeper end of the zone where in situ production is purported to occur (Sinninghe Damsté, 2016), suggesting that in situ production indeed changes at depths >~300 m. However, it remains unclear whether the brGDGT production takes place in the water column or in the sediment itself (Sinninghe Damsté, 2016). In contrast, the lowest #rings$_{tetra}$ values occur in the inner fjords (average 0.72), and may be the result of the input of soil material with lower #rings$_{tetra}$ by glaciers (Winkelmann and Knies, 2005; Peterse et al., 2009). Indeed, the slightly higher BIT (0.05) and the more soil-like distribution of brGDGTs in the sediment station in front of the Kronebreen glacier in Kongsfjorden (NP08-16-64) compared to the even lower BIT at all other sites (Supplementary Table S1) were previously used as evidence for the input of soil material (station NP07-13-61 in Peterse et al., 2009).

The spatial pattern of #rings$_{tetra}$ based on IPL-derived brGDGTs (0.24–0.79) is broadly similar to that of the CLs (0.65–0.93), except that the spread in #rings$_{tetra}$ is much larger (Fig. 4C). Interestingly, plotting the offset between the #rings$_{tetra}$ between the CL and IPL-derived brGDGTs indicates that the IPL-derived brGDGTs and CL signals are more comparable in the fjords than at the mouth of the fjords or towards the open ocean, where the discrepancy can be up to 0.52 (Fig. 4D). One environmental parameter that follows a similar gradient is salinity, which is generally lower in the fjords due to the input of glacial meltwater, and increases towards the open ocean (Promińska et al., 2017; Jernas et al., 2018; Supplementary Table S2). The salinity gradient is most pronounced in the summer months due to the interaction between the tidewater glaciers, and the inflow of warm, saline Atlantic Water (Jernas et al., 2018). The spatial pattern of #rings$_{tetra}$ of IPL-brGDGTs (Fig. 4C) then suggests that the incorporation of cyclopentane moieties may be linked to decreasing salinity. At the time of sampling (August 2008), the surface salinity is ~32 g kg^{-1} in the inner and central parts of Kongsfjorden and increases to 34 g kg^{-1} at the outer fjord and shelf area (Supplementary Table S2). The vertical depth gradient shows that the salinity increases to values of 35 g kg^{-1} at depths ~50 m (at 50–100 m for the inner parts of the fjords; Jernas et al., 2018). However, the surface salinity gradient as well as the vertical salinity gradient changes throughout and among years, depending on the unpredictable input of Atlantic Water to Kongsfjorden (Jernas et al., 2018). Hence, there is no clear correlation between sea surface salinity at the time of sampling (Supplementary Table S2) and #rings$_{tetra}$ of the IPL-derived brGDGTs ($R^2 = 0.19$, $p = 0.16$). Only upon removal of the station closest to the Kronebreen glacier (NP08-16-64; with presumed increased terrestrial influence), a correlation becomes apparent ($R^2 = 0.41$, $p = 0.016$), although #rings$_{tetra}$ then respond to sea surface temperature as well ($R^2 = 0.33$, $p = 0.033$). It thus remains difficult to attribute the change in #rings$_{tetra}$ in the 'living' brGDGTs to salinity, temperature, or both.

Interestingly, the bacterial community in sediments close to the Kronebreen glacier terminus also differs from that in sediments influenced by seawater (Conte et al., 2018). Close to the glacier terminus, the bacterial community in the fjord mainly consists of Chloroflexi, Acidobacteria, and Nitrospirae, whereas Proteobacteria, Parcubacteria, Firmicutes, and Actinobacteria become more abundant towards the open ocean (Conte et al., 2018). Of these bacterial phyla, only Acidobacteria are so far purported to produce brGDGTs (brGDGT-Ia in particular; Sinninghe Damsté et al., 2011, 2018). However, other bacterial groups may also produce brGDGTs, and a shift in bacterial communities may thus explain the simultaneous changes in the #rings$_{tetra}$ of the IPL-derived brGDGTs. Alternatively, the same bacterial community may be influenced by the salinity gradient, leading to membrane adaptation where more rings are incorporated at lower salinity, and vice versa. This may be a similar process to bacteria that experience acid stress that introduce cyclopropane rings in their alkyl chains to increase stability (Zhang and Rock, 2008). Despite the limited knowledge of brGDGT producers, in order to investigate the effect of these parameters further, a mesocosm study where temperature and salinity are varied in a controlled manner may be a step forward in constraining the effect of these environmental parameters on brGDGT distributions in aquatic systems.
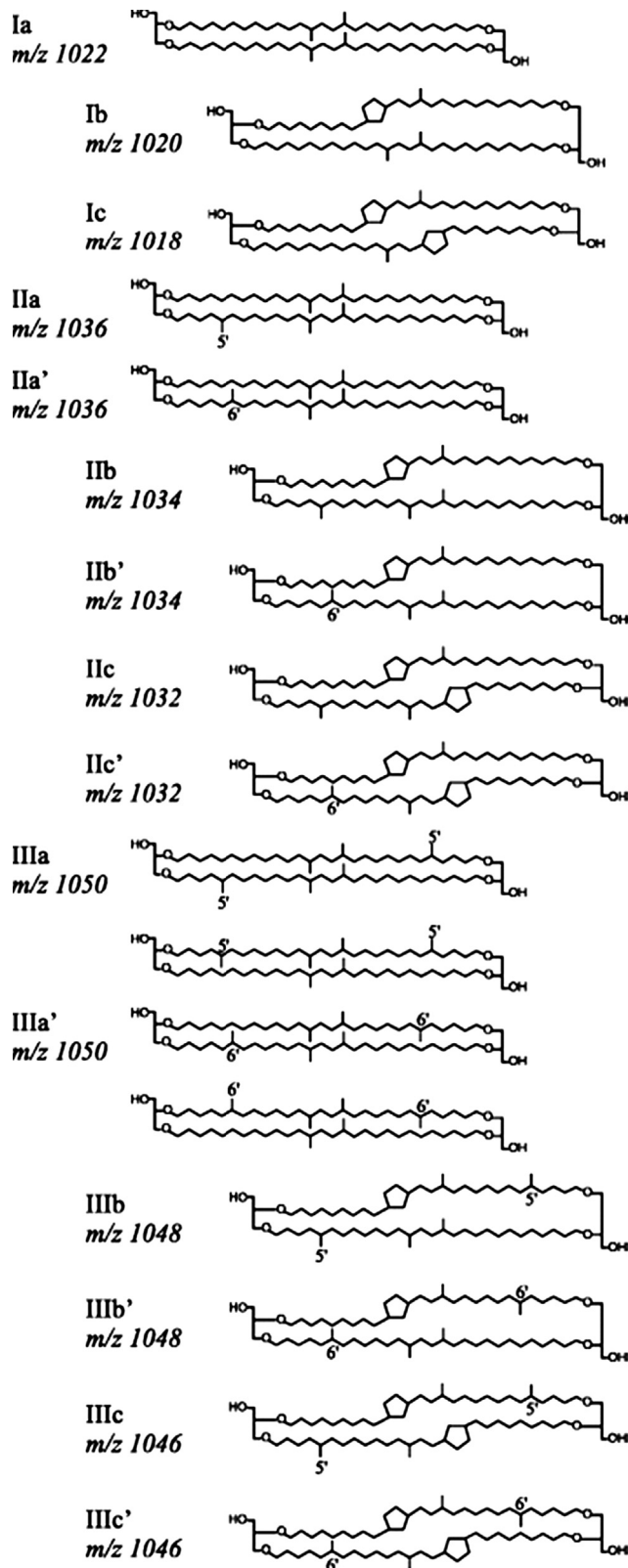
5. Conclusions

BrGDGT distributions indicate that 6-methyl brGDGTs are important brGDGTs in Svalbard soils. Subsequent comparison with brGDGT distributions in fjord sediments confirms the earlier conclusion of Peterse et al. (2009) and Sinninghe Damsté (2016) that most brGDGTs in the fjord sediments are produced in situ and are characterized by a high degree of cyclisation of both tetra- and pentamethylated compounds. In particular, the #rings$_{tetra}$ of the IPL-derived brGDGTs in the fjord sediments show a large range of variation, whereas the #rings$_{penta}$ remains relatively constant. The subsequent discrepancy in #rings$_{tetra}$ values (up to a difference of 0.52) between the IPL-derived brGDGTs and CLs in the same sediment indicates that brGDGTs in Svalbard are produced in seasonally varying distributions throughout the year. Furthermore, the increasing offset between #rings$_{tetra}$ in CLs and IPL-derived brGDGTs from the inner fjord towards the open marine environment points toward a possible salinity and/or temperature influence on marine brGDGT production. This indicates that membrane adaptation to increasing/decreasing salinity and/or temperature may be responsible for the degree of cyclisation of aquatically produced tetramethylated brGDGTs, or that the microbial community of brGDGT-producing bacteria changes on the glacio-marine transect.

Acknowledgements

Appendix A

Molecular structures of the tetramethylated (Ia–Ic), pentamethylated (IIa–IIc), and hexamethylated (IIIa–IIIc) brGDGTs, where 6-methyl isomers are indicated with a prime symbol.

Appendix B. Supplementary material

Supplementary data to this article can be found online at https://doi.org/10.1016/j.orggeochem.2019.103907.

Associate Editor—**Isla S. Castañeda**

References

Ballantyne, A.P., Greenwood, D.R., Sinninghe Damsté, J.S., Csank, A.Z., Eberle, J.J., Rybczynski, N., 2010. Significantly warmer Arctic surface temperatures during the Pliocene indicated by multiple independent proxies. Geology 38, 603–606.

Birks, H.J.B., Jones, V.J., Rose, N.L., 2004. Recent environmental change and atmospheric contamination on Svalbard as recorded in lake sediments–synthesis and general conclusions. Journal of Paleolimnology 31, 531–546.

Conte, A., Papale, M., Amalfitano, S., Mikkonen, A., Rizzo, C., De Domenico, E., Michaud, L., Lo Giudice, A., 2018. Bacterial community structure along the subtidal sandy sediment belt of a high Arctic fjord (Kongsfjorden, Svalbard Islands). Science of the Total Environment 619–620, 203–211.

De Jonge, C., Hopmans, E.C., Stadnitskaia, A., Rijpstra, W.I.C., Hofland, R., Tegelaar, E., Sinninghe Damsté, J.S., 2013. Identification of novel penta- and hexamethylated branched glycerol dialkyl glycerol tetraethers in peat using HPLC–MS^2, GC–MS and GC–SMB-MS. Organic Geochemistry 54, 78–82.

De Jonge, C., Hopmans, E.C., Zell, C.I., Kim, J.H., Schouten, S., Sinninghe Damsté, J.S., 2014a. Occurrence and abundance of 6-methyl branched glycerol dialkyl glycerol tetraethers in soils: Implications for palaeoclimate reconstruction. Geochimica et Cosmochimica Acta 141, 97–112.

De Jonge, C., Stadnitskaia, A., Hopmans, E.C., Cherkashov, G., Fedotov, A., Sinninghe Damsté, J.S., 2014b. In situ produced branched glycerol dialkyl glycerol tetraethers in suspended particulate matter from the Yenisei River, Eastern Siberia. Geochimica et Cosmochimica Acta 125, 476–491.

De Jonge, C., Stadnitskaia, A., Hopmans, E.C., Cherkashov, G., Fedotov, A., Streletskaya, I.D., Vasiliev, A.A., Sinninghe Damsté, J.S., 2015. Drastic changes in the distribution of branched tetraether lipids in suspended matter and sediments from the Yenisei River and Kara Sea (Siberia): Implications for the use of brGDGT-based proxies in coastal marine sediments. Geochimica et Cosmochimica Acta 165, 200–225.

Dearing, Crampton-Flood E., Peterse, F., Munsterman, D., Sinninghe Damsté, J.S., 2018. Using tetraether lipids archived in North Sea Basin sediments to extract North Western European Pliocene continental air temperatures. Earth and Planetary Science Letters 490, 193–205.

Ding, S., Schwab, V.F., Ueberschaar, N., Roth, V.N., Lange, M., Xu, Y., Gleixner, G., Pohnert, G., 2016. Identification of novel 7-methyl and cyclopentanyl branched glycerol dialkyl glycerol tetraethers in lake sediments. Organic Geochemistry 102, 52–58.

Herfort, L., Schouten, S., Boon, J.P., Woltering, M., Baas, M., Weijers, J.W., Sinninghe Damsté, J.S., 2006. Characterization of transport and deposition of terrestrial organic matter in the southern North Sea using the BIT index. Limnology and Oceanography 51, 2196–2205.

Hop, H., Pearson, T., Hegseth, E.N., Kovacs, K.M., Wiencke, C., Kwasniewski, S., Eiane, K., Mehlum, F., Gulliksen, B., Wlodarska-Kowalczuk, M., Lydersen, C., 2002. The marine ecosystem of Kongsfjorden, Svalbard. Polar Research 21, 167–208.

Hopmans, E.C., Weijers, J.W., Schefuß, E., Herfort, L., Sinninghe Damsté, J.S., Schouten, S., 2004. A novel proxy for terrestrial organic matter in sediments based on branched and isoprenoid tetraether lipids. Earth and Planetary Science Letters 224, 107–116.

Hopmans, E.C., Schouten, S., Sinninghe Damsté, J.S., 2016. The effect of improved chromatography on GDGT-based palaeoproxies. Organic Geochemistry 93, 1–6.

Huguet, C., Hopmans, E.C., Febo-Ayala, W., Thompson, D.H., Sinninghe Damsté, J.S., Schouten, S., 2006. An improved method to determine the absolute abundance of glycerol dibiphytanyl glycerol tetraether lipids. Organic Geochemistry 37, 1036–1041.

Inglis, G.N., Collinson, M.E., Riegel, W., Wilde, V., Farnsworth, A., Lunt, D.J., Valdes, P., Robson, B.E., Scott, A.C., Lenz, O.K., Naafs, B.D.A., 2017. Mid-latitude continental temperatures through the early Eocene in western Europe. Earth and Planetary Science Letters 460, 86–96.

Jernas, P., Klitgaard-Kristensen, D., Husum, K., Koç, N., Tverberg, V., Loubere, P., Prins, M., Dijkstra, N., Gluchowska, M., 2018. Annual changes in Arctic fjord environment and modern benthic foraminiferal fauna: Evidence from Kongsfjorden, Svalbard. Global and Planetary Change 163, 119–140.

Keisling, B.A., Castañeda, I.S., Brigham-Grette, J., 2017. Hydrological and temperature change in Arctic Siberia during the intensification of Northern Hemisphere Glaciation. Earth and Planetary Science Letters 457, 136–148.

Kim, J.H., Schouten, S., Buscail, R., Ludwig, W., Bonnin, J., Sinninghe Damsté, J.S., Bourrin, F., 2006. Origin and distribution of terrestrial organic matter in the NW Mediterranean (Gulf of Lions): Exploring the newly developed BIT index. Geochemistry, Geophysics, Geosystems 7. https://doi.org/10.1029/2006GC001306.

Kim, J.H., Ludwig, W., Schouten, S., Kerhervé, P., Herfort, L., Bonnin, J., Sinninghe Damsté, J.S., 2007. Impact of flood events on the transport of terrestrial organic matter to the ocean: a study of the Têt River (SW France) using the BIT index. Organic Geochemistry 38, 1593–1606.

Koga, Y., Nishihara, M., Morii, H., Akagawa-Matsushita, M., 1993. Ether polar lipids of methanogenic bacteria: structures, comparative aspects, and biosyntheses. Microbiology and Molecular Biology Reviews 57, 164–182.

Lengger, S.K., Hopmans, E.C., Sinninghe Damsté, J.S., Schouten, S., 2012. Comparison of extraction and work up techniques for analysis of core and intact polar tetraether lipids from sedimentary environments. Organic Geochemistry 47, 34–40.

Liu, X.L., Zhu, C., Wakeham, S.G., Hinrichs, K.-U., 2014. In situ production of branched glycerol dialkyl glycerol tetraethers in anoxic marine water columns. Marine Chemistry 166, 1–8.

Naafs, B.D.A., Inglis, G.N., Zheng, Y., Amesbury, M.J., Biester, H., Bindler, R., Blewett, J., Burrows, M.A., del Castillo Torres, D., Chambers, F.M., Cohen, A.D., 2017a. Introducing global peat-specific temperature and pH calibrations based on brGDGT bacterial lipids. Geochimica et Cosmochimica Acta 208, 285–301.

Naafs, B.D.A., Gallego-Sala, A.V., Inglis, G.N., Pancost, R.D., 2017b. Refining the global branched glycerol dialkyl glycerol tetraether (brGDGT) soil temperature calibration. Organic Geochemistry 106, 48–56.

Naafs, B.D.A., Rohrssen, M., Inglis, G.N., Lähteenoja, O., Feakins, S.J., Collinson, M.E., Kennedy, E.M., Singh, P.K., Singh, M.P., Lunt, D.J., Pancost, R.D., 2018. High temperatures in the terrestrial mid-latitudes during the early Palaeogene. Nature Geoscience 11, 766–771.

Peterse, F., Kim, J.H., Schouten, S., Kristensen, D.K., Koç, N., Sinninghe Damsté, J.S., 2009. Constraints on the application of the MBT/CBT palaeothermometer at high latitude environments (Svalbard, Norway). Organic Geochemistry 40, 692–699.

Peterse, F., van der Meer, J., Schouten, S., Weijers, J.W., Fierer, N., Jackson, R.B., Kim, J.H., Sinninghe Damsté, J.S., 2012. Revised calibration of the MBT–CBT paleotemperature proxy based on branched tetraether membrane lipids in surface soils. Geochimica et Cosmochimica Acta 96, 215–229.

Pitcher, A., Hopmans, E.C., Schouten, S., Sinninghe Damsté, J.S., 2009. Separation of core and intact polar archaeal tetraether lipids using silica columns: insights into living and fossil biomass contributions. Organic Geochemistry 40, 12–19.

Promińska, A., Cisek, M., Walczowski, W., 2017. Kongsfjorden and Hornsund hydrography–comparative study based on a multiyear survey in fjords of west Spitsbergen. Oceanologia 59, 397–412.

Sinninghe Damsté, J.S., 2016. Spatial heterogeneity of sources of branched tetraethers in shelf systems: the geochemistry of tetraethers in the Berau River delta (Kalimantan, Indonesia). Geochimica et Cosmochimica Acta 186, 13–31.

Sinninghe Damsté, J.S., Hopmans, E.C., Pancost, R.D., Schouten, S., Geenevasen, J., 2000. Newly discovered non-isoprenoid dialkyl diglycerol tetraether lipids in sediments. Journal of the Chemical Society, Chemical Communications, 1683–1684.

Sinninghe Damsté, J.S., Ossebaar, J., Abbas, B., Schouten, S., Verschuren, D., 2009. Fluxes and distribution of tetraether lipids in an equatorial African lake: constraints on the application of the TEX$_{86}$ palaeothermometer and BIT index in lacustrine settings. Geochimica et Cosmochimica Acta 73, 4232–4249.

Sinninghe Damsté, J.S., Rijpstra, W.I.C., Hopmans, E.C., Weijers, J.W., Foesel, B.U., Overmann, J., Dedysh, S.N., 2011. 13,16-Dimethyl octacosanedioic acid (iso-diabolic acid): A common membrane-spanning lipid of Acidobacteria subdivisions 1 and 3. Applied and Environmental Microbiology 77, 4147–4154.

Sinninghe Damsté, J.S., Rijpstra, W.I.C., Hopmans, E.C., Foesel, B.U., Wüst, P.K., Overmann, J., Tank, M., Bryant, D.A., Dunfield, P.F., Houghton, K., Stott, M.B., 2014. Ether- and ester-bound iso-diabolic acid and other lipids in members of Acidobacteria subdivision 4. Applied and Environmental Microbiology 80, 5207–5218.

Sinninghe Damsté, J.S., Rijpstra, W.I.C., Foesel, B.U., Huber, K.J., Overmann, J., Nakagawa, S., Kim, J.J., Dunfield, P.F., Dedysh, S.N., Villanueva, L., 2018. An overview of the occurrence of ether- and ester-linked iso-diabolic acid membrane lipids in microbial cultures of the Acidobacteria: Implications for brGDGT paleoproxies for temperature and pH. Organic Geochemistry 124, 63–76.

Svendsen, H., Beszczynska-Møller, A., Hagen, J.O., Lefauconnier, B., Tverberg, V., Gerland, S., Børre Ørbæk, J., Bischof, K., Papucci, C., Zajaczkowski, M., Azzolini, R., 2002. The physical environment of Kongsfjorden-Krossfjorden, an Arctic fjord system in Svalbard. Polar Research 21, 133–166.

Tierney, J.E., Russell, J.M., 2009. Distributions of branched GDGTs in a tropical lake system: Implications for lacustrine application of the MBT/CBT paleoproxy. Organic Geochemistry 40, 1032–1036.

Warden, L., Moros, M., Weber, Y., Sinninghe Damsté, J.S., 2018. Change in provenance of branched glycerol dialkyl glycerol tetraethers over the Holocene in the Baltic Sea and its impact on continental climate reconstruction. Organic Geochemistry 121, 138–154.

Weber, Y., De Jonge, C., Rijpstra, W.I.C., Hopmans, E.C., Stadnitskaia, A., Schubert, C.J., Lehmann, M.F., Sinninghe Damsté, J.S., Niemann, H., 2015. Identification and carbon isotope composition of a novel branched GDGT isomer in lake sediments: Evidence for lacustrine branched GDGT production. Geochimica et Cosmochimica Acta 154, 118–129.

Weber, Y., Sinninghe Damsté, J.S., Zopfi, J., De Jonge, C., Gilli, A., Schubert, C.J., Lepori, F., Lehmann, M.F., Niemann, H., 2018. Redox-dependent niche differentiation provides evidence for multiple bacterial sources of glycerol tetraether lipids in lakes. Proceedings of the National Academy of Sciences 115, 10926–10931.

Weijers, J.W., Schouten, S., van den Donker, J.C., Hopmans, E.C., Sinninghe Damsté, J. S., 2007a. Environmental controls on bacterial tetraether membrane lipid distribution in soils. Geochimica et Cosmochimica Acta 71, 703–713.

Weijers, J.W., Schefuß, E., Schouten, S., Sinninghe Damsté, J.S., 2007b. Coupled thermal and hydrological evolution of tropical Africa over the last deglaciation. Science 315, 1701–1704.

Weijers, J.W., Schouten, S., Sluijs, A., Brinkhuis, H., Sinninghe Damsté, J.S., 2007c. Warm arctic continents during the Palaeocene-Eocene thermal maximum. Earth and Planetary Science Letters 261, 230–238.

Weijers, J.W., Bernhardt, B., Peterse, F., Werne, J.P., Dungait, J.A., Schouten, S., Sinninghe Damsté, J.S., 2011. Absence of seasonal patterns in MBT–CBT indices in mid-latitude soils. Geochimica et Cosmochimica Acta 75, 3179–3190.

Weijers, J.W., Schefuß, E., Kim, J.H., Sinninghe Damsté, J.S., Schouten, S., 2014. Constraints on the sources of branched tetraether membrane lipids in distal marine sediments. Organic Geochemistry 72, 14–22.

White, D.C., Davis, W.M., Nickels, J.S., King, J.D., Bobbie, R.J., 1979. Determination of the sedimentary microbial biomass by extractible lipid phosphate. Oecologia 40, 51–62.

Winkelmann, D., Knies, J., 2005. Recent distribution and accumulation of organic carbon on the continental margin west off Spitsbergen. Geochemistry, Geophysics, Geosystems 6. https://doi.org/10.1029/2005GC000916.

Xie, S., Liu, X.L., Schubotz, F., Wakeham, S.G., Hinrichs, K.U., 2014. Distribution of glycerol ether lipids in the oxygen minimum zone of the Eastern Tropical North Pacific Ocean. Organic Geochemistry 71, 60–71.

Zell, C., Kim, J.H., Moreira-Turcq, P., Abril, G., Hopmans, E.C., Bonnet, M.P., Sobrinho, R.L., Sinninghe Damsté, J.S., 2013a. Disentangling the origins of branched tetraether lipids and crenarchaeol in the lower Amazon River: Implications for GDGT-based proxies. Limnology and Oceanography 58, 343–353.

Zell, C., Kim, J.H., Abril, G., Sobrinho, R., Dorhout, D., Moreira-Turcq, P., Sinninghe Damsté, J., 2013b. Impact of seasonal hydrological variation on the distributions of tetraether lipids along the Amazon River in the central Amazon basin: Implications for the MBT/CBT paleothermometer and the BIT index. Frontiers in Microbiology 4, 228.

Zell, C., Kim, J.H., Balsinha, M., Dorhout, D., Fernandes, C., Baas, M., Sinninghe Damsté, J.S., 2014a. Transport of branched tetraether lipids from the Tagus River basin to the coastal ocean of the Portuguese margin: Consequences for the interpretation of the MBT'/CBT paleothermometer. Biogeosciences 11, 5637–5655.

Zell, C., Kim, J.H., Hollander, D., Lorenzoni, L., Baker, P., Silva, C.G., Nittrouer, C., Sinninghe Damsté, J.S., 2014b. Sources and distributions of branched and isoprenoid tetraether lipids on the Amazon shelf and fan: Implications for the use of GDGT-based proxies in marine sediments. Geochimica et Cosmochimica Acta 139, 293–312.

Zell, C., Kim, J.H., Dorhout, D., Baas, M., Sinninghe Damsté, J.S., 2015. Sources and distributions of branched tetraether lipids and crenarchaeol along the Portuguese continental margin: Implications for the BIT index. Continental Shelf Research 96, 34–44.

Zhang, Y.M., Rock, C.O., 2008. Membrane lipid homeostasis in bacteria. Nature Reviews Microbiology 6, 222.

Zhu, C., Weijers, J.W., Wagner, T., Pan, J.M., Chen, J.F., Pancost, R.D., 2011. Sources and distributions of tetraether lipids in surface sediments across a large river-dominated continental margin. Organic Geochemistry 42, 376–386.

Zhu, R., Ding, W., Hou, L., Wang, Q., 2014. Matrix-bound phosphine and phosphorus fractions in surface sediments of Arctic Kongsfjorden, Svalbard: effects of glacial activity and environmental variables. Chemosphere 103, 240–249.